Scalable Single-Step Noninjection Synthesis of High-Quality Core/Shell Quantum Dots with Emission Tunable from Violet to Near Infrared

Wenjin Zhang, Hua Zhang, Yaoyu Feng, and Xinhua Zhong*

State Key Laboratory of Bioreactor Engineering, Institute of Applied Chemistry, East China University of Science and Technology, Shanghai 200237, China

ABSTRACT The common two-step "hot-injection" methods are not suitable for reproducible production of core/shell quantum dots (QDs) at large scale for practical applications. Herein we develop a scalable, reproducible, and low-cost synthetic approach for high-quality core/shell QDs ($CdS/Zn_xCd_{1-x}S$, $CdSe/Zn_xCd_{1-x}S$, and $CdTe/Zn_xCd_{1-x}S$) with shell material composed of gradient alloy structure by directly heating commercial available, air-stable CdO, $Zn(NO_3)_2$, and chalcogenide elements in octadecene media at air. With simple variation of reaction recipe (reactants and feeding ratio), luminescence color of the resulting QDs can be conveniently tuned from violet to near-infrared (400–820 nm). The emission efficiency of the as-prepared QDs can be up to 80%. Moreover, the high emission efficiency can be preserved after QDs transferred into aqueous media *via* ligand exchange. The structure, chemical composition, and optical properties of the obtained QDs have been characterized with use of transmission electron microscopy, elemental analysis, and optical spectroscopy. The scalability of the reported approach has been demonstrated by the facile preparation of gram-scaled QD product in one batch reaction.

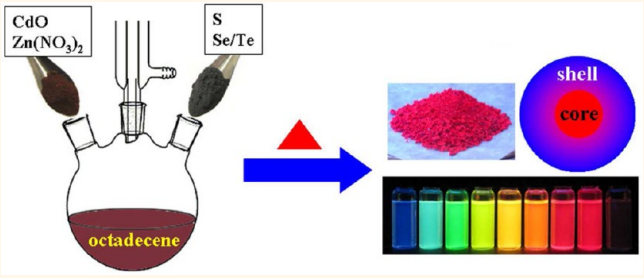

KEYWORDS: scalable synthesis · one-pot noninjection synthesis · quantum dots · photoluminescence

With the growing interest in applications ranging from health (biolabeling/imaging) to energy (photovoltaics and light emitting diodes) based on semiconductor nanocrystals (also termed as quantum dots, QDs) comes a need for highly reproducible, large-scale synthesis of these materials with uniform size and shape, narrow emission peak, high photoluminescence quantum yield (PL QY), and high photo- and chemical stability.[1–6] It is known that as-prepared binary II–VI QDs is not stable enough and sensitive to processing conditions and environments, which are detrimental for the practical application of QD in various areas.[7–9] To combat these disadvantages, recent efforts have focused on the development of core/shell QDs *via* epitaxially overcoating a shell of wider band gap semiconductor materials around the core QDs.[10–26] Commonly, core/shell QDs are fabricated *via* a two-step procedure: initial synthesis of core QDs, mostly relying on "hot-injection method" by rapid injection of precursors into hot reaction media,[27–36] followed by the shell growth reaction *via* either dropwise or successive ion layer adsorption reaction method.[10–26] Unfortunately, both the hot-injection-based synthetic method for core nanocrystals and the shell deposition procedure are not suitable for large-scale preparation (e.g., hundreds of kilograms), even though it can be scaled up to the order of grams.[7,37,38] In addition, high cost and harsh operation conditions are also reasons that impede the practical application of QDs. The essential components in the synthesis of core/shell QDs typically include expensive, pyrophoric, and toxic tertiary phosphine chalcogenides, hexamethyldisilathiane, and organometallic compounds (such as $CdMe_2$, $ZnEt_2$) as the reactive precursors. This renders the synthesis of core/shell QDs usually expensive, labor-intensive, and time-consuming. It is highly desirable that synthetic

* Address correspondence to zhongxh@ecust.edu.cn.

Received for review October 15, 2012 and accepted November 24, 2012.

Published online December 12, 2012
10.1021/nn304765k

methods that are aimed at producing high-quality core/shell QDs for potential applications are scalable, reproducible, environmentally friendly, and low cost.

Noninjection, or heating-up method, wherein all reagents are loaded in a single reaction pot at room temperature and subsequent heated to reflux for nanocrystals nucleation and growth, is a promising route to large-scale preparation due to the absence of precursor injection.[39−42] To our best knowledge, there are few reports for the synthesis of II−VI group core/shell QDs with use of single-step noninjection method though this method has been extensively employed in the preparation of metal oxides,[43] noble metals,[44] and occasionally in plain binary core QDs.[40,45] Herein, we report a scalable single-step noninjection synthetic approach for high-quality core/shell QDs (CdS/$Zn_xCd_{1-x}S$, CdSe/$Zn_xCd_{1-x}S$, and CdTe/$Zn_xCd_{1-x}S$) with shell material composed of gradient alloy structure by directly heating commercial available, air-stable CdO, $Zn(NO_3)_2$, and chalcogenide elements in octadecene (ODE) media at air (Figure 1). With variation of reactants and feeding ratio, the luminescence color of the resulting QDs can be conveniently tuned from violet to near-infrared (NIR; 400−820 nm). The PL QY of the as-prepared QDs can be up to 80%. Moreover, the high QY can be preserved after QDs transferred into aqueous media *via* ligand exchange. This facile single-step noninjection strategy provides a versatile route to low-cost, reproducible and large-scale preparation of high-quality core/shell QDs with interested emission colors for practical applications.

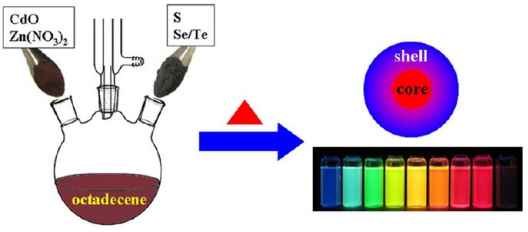

Figure 1. Overall scheme for the single-step noninjection synthesis of core/shell QDs.

RESULTS AND DISCUSSION

Optical Properties. Synthesis of CdSe/$Zn_xCd_{1-x}S$ QDs with emission wavelength around 625 nm is chosen as an example to demonstrate this single-step noninjection approach in preparation of high-quality core/shell QDs, and the detailed procedures are described in Materials and Methods. Briefly, CdO, $Zn(NO_3)_2$, Se, and S were loaded in ODE media containing trioctylphosphine (TOP) and stearic acid (SA) at room temperature and then heated to 250 °C at air under stirring. Figure 2a shows the temporal evolution of UV−vis absorption and PL emission spectra of the as-prepared QDs under growth temperature of 250 °C. Both the sharp excitonic absorption peak in the absorption spectra and the symmetric and narrow band edge PL emission peak (with full width at half-maximum in the range of 27−31 nm) in the PL spectra indicate the fact that particle size and shape are nearly uniform. Figure 2b summarizes the PL peak position and PL QYs of the obtained QDs under different growth times. With the reaction temperature approaching 250 °C, QDs with PL emission wavelength of about 600 nm was obtained. This indicates fast nucleation and crystal growth in the heating-up process. In the following course of 2 h growth/annealing, the PL peak position shifted from 600 to 625 nm and the PL QY increased quickly and got near to the maximum value of 81% after 30 min, which is one of the best results in the red light window for the CdSe based QDs,[36] and this high QY can be kept for the next 2 h. The observed long-term fixation of emission wavelength indicates that there is almost no change in particle size and chemical composition for the obtained QDs. This may be derived from the characteristic hardened lattice structure of the gradient alloy in the shell materials. This phenomenon has also been observed in the $Zn_xCd_{1-x}Se$ alloyed QD system.[45] The feature of long-term fixation of PL peak position and PL brightness is favorable for the reproducible synthesis of luminescent QDs with desired optical properties as discussed below.

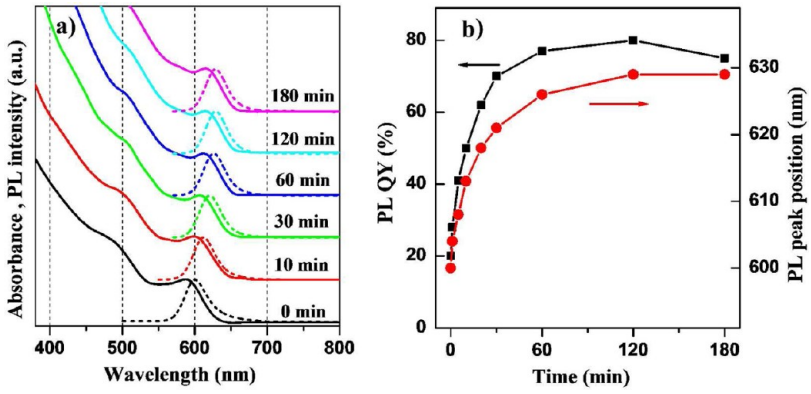

Figure 2. (a) Temporal evolution of UV−vis (solid lines) and PL (dashed lines, λ_{ex} = 350 nm) spectra of CdSe/$Zn_xCd_{1-x}S$ QDs grown at 250 °C. (b) Summary of PL peak positions and QYs of the obtained QDs under different growth times.

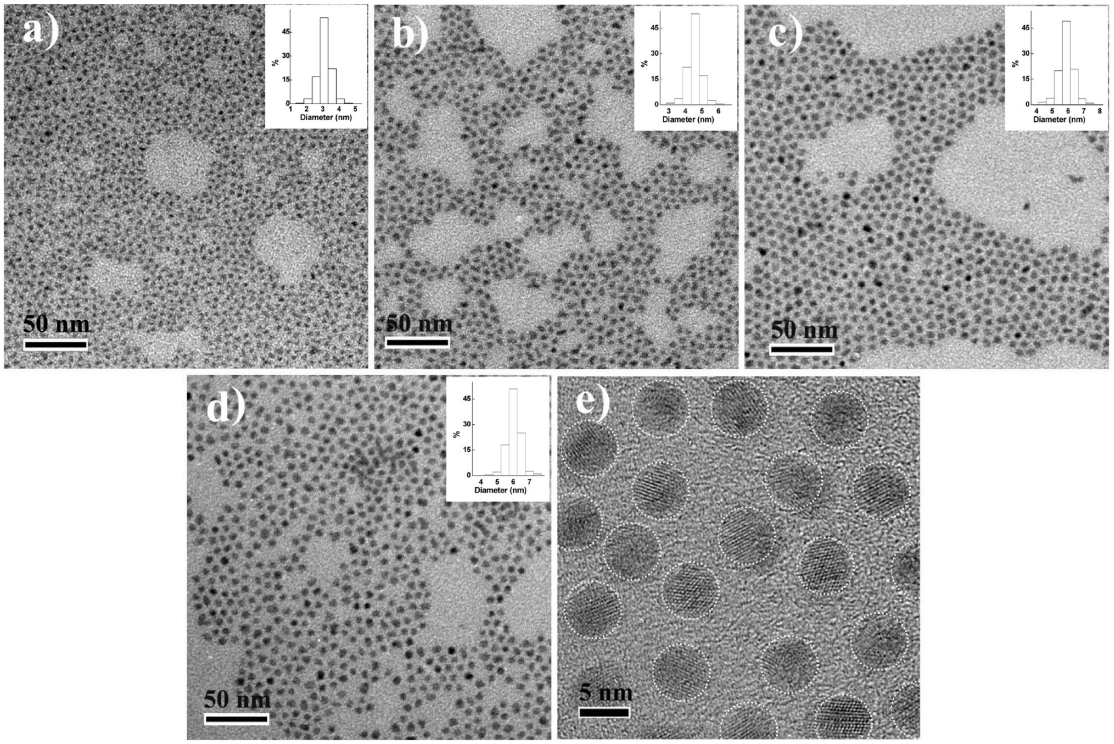

Figure 3. Wide-field TEM images of CdSe/$Zn_xCd_{1-x}S$ QD samples taken at 170 °C (a) and at 250 °C with growth time of 0 min (b), 30 min (c), and 2 h (d). (e) HRTEM images of sample d. Insets are the corresponding histograms of the size distribution.

Structure Characterization. To monitor the particle growth process, aliquots of samples at the initial formation stage corresponding to reaction temperature of 170 °C together with samples at growth temperature of 250 °C for different times were taken and transmission electron microscopy (TEM) measurements were carried out. The wide-field TEM images of representative samples taken at 170 °C together with at 250 °C for different growth times are shown in Figure 3. At different growth stages, all the as-prepared QDs display a nearly spherical shape with mean size increasing from 3.1 ± 0.2 nm (at 170 °C), 4.6 ± 0.3 nm (0 min at 250 °C), to 5.9 ± 0.3 nm (30 min at 250 °C), and 6.1 ± 0.3 nm (2 h at 250 °C) as the reaction proceeded. All the samples of the as-prepared nanocrystals have a narrow size distribution with a relative standard deviation (σ) of 6−7% without any postpreparation fractionation or size sorting, and the corresponding histograms of size distribution based on analytical results of more than 200 particles in a given area are given in insets of Figure 3. The high-resolution TEM images (Figure 3e) of the obtained QDs reveal a uniform spherical shape with well-resolved lattice fringes, demonstrating the highly crystalline nature of the nanocrystals. The typical X-ray diffraction (XRD) pattern of the obtained QDs (Figure S1 in Supporting Information, SI) consists of the characterized peaks of cubic zinc blende CdSe, but the position of diffraction peaks is located between CdSe and ZnS.

TABLE 1. Atomic % of the Elements Determined from ICP-AES Analysis (Mean Values of 5 Independent Measurements per Sample) for Samples at Different Reaction Stages

reaction stages	Cd	Zn	Zn/(Zn + Cd)	Se	S	S/(S + Se)
170 °C	100	0.33	0	98.5	0.21	0
0 min	100	8.2	0.08	86.2	20.9	0.2
30 min	100	25.1	0.2	47.3	77.4	0.62
60 min	100	28.6	0.22	44.3	84.4	0.65
120 min	100	29.5	0.23	44.2	85.9	0.66

Chemical Composition Analysis. To identify the chemical composition of the QDs, conductively coupled plasma atomic emission spectroscopy (ICP-AES) analyses for the representative samples as shown in Figure 3 were recorded (Table 1), and the molar ratios of Zn/(Cd + Zn), and S/(Se + S) based on ICP data are summarized in Figure 4. At the early reaction stage (at 170 °C), almost no Zn and S were detected in the samples and thus the composition of the QD can deduce to be nearly plain CdSe. This indicates that, at the experimental conditions, the reactivity of Cd is higher than that of Zn and the same situation for Se to S. This finding is consistent with previous observations.[46−48] This renders the successful decoupling of core growth and shell deposition and results in the formation of core/shell structure. With proceeding of QDs growth, the Zn/(Zn + Cd) and S/(S + Se) ratios increased steadily and become constant with the values of 0.22 and 0.66, respectively, after 1 h. The time period for the

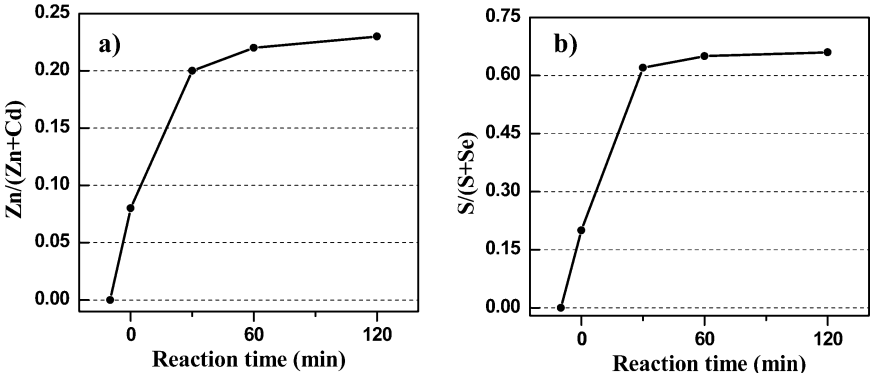

Figure 4. Composition ratios of Zn/(Zn + Cd) (a) and S/(S + Se) (b) at different reaction stages. The first points correspond to sample taken at 170 °C.

fixation of chemical composition is consistent with that for the fixation of PL peak position as described above. The fixation of PL peak position indicates the fact that intraparticle atomic diffusion is negligible for the CdSe/$Zn_xCd_{1-x}S$ system during the annealing process at 250 °C. This observation is in accordance with previous result that alloying process can be neglected at temperature less than 250 °C for 6 nm CdSe/ZnSe core/shell system.[49] The increase of Zn and S concentration in the obtained QD system could be ascribed to the enhancement of reactivity of Zn and S precursors due to the increase of reaction temperature, and to the decrease of concentrations of Cd/Se precursors due to formation of CdSe core nanocrystals. The temporal evolution of chemical composition indicates that the core is composed of Cd and Se, the outer shell is composed of Cd, Zn, and S, but the amounts of Cd and Se decrease radially outward, while the amounts of Zn and S increase. Therefore, the formed QD is a pseudo core/shell structure with the shell material composed of a gradient $Zn_xCd_{1-x}S$ alloy, as shown in Figure 1. Similar gradient alloy structures have been reported in previous literature.[48,50,51] It should be noted that partially alloying process should be possible to take place between the core and shell interface and, thus, the clear core, shell interface is difficult to be observed by the TEM analysis. For simplicity, a core/shell structure was termed hereafter. The gradient $Zn_xCd_{1-x}S$ alloy shell layer relieves efficiently interface strain caused by the lattice mismatch between CdSe and ZnS and thus favors the high PL QYs.[11,17] The energy-dispersive X-ray (EDX) spectra of a typical sample with growth time of 0.5 h at 250 °C (Figure S2) also confirm the presence of Cd, Zn, Se, and S in the sample.

Effect of Nature of Reactants. To understand the mechanism for formation of monodisperse core/shell nanocrystals, we investigated the nature of reactants on the effect of the obtained QDs. In the reported single-step noninjection approach (denoted as R_0), CdO, $Zn(NO_3)_2$, elemental Se and S were used directly as metal and chalcogenide sources, respectively.

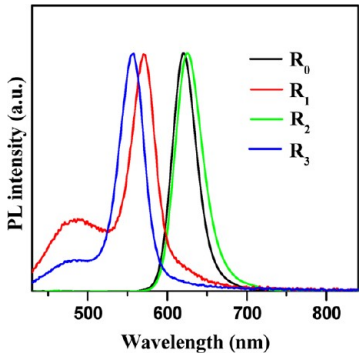

Figure 5. Dependence of PL feature of obtained QDs on the nature of reactants: in R_0, CdO, S, and Se as reactants; in R_1, activated CdO as Cd source; in R_2, activated Se and S as reactants; in R_3, activated Cd, S, and Se used.

In control experiments (R_1–R_3), activated Cd source (cadmium stearate), and/or activated Se, S sources (TOP-Se, TOP-S) were adopted. Experimental results (Figure 5) indicate that the adoption of CdO as Cd source is critical for the formation of monodisperse core/shell QDs with narrow and symmetric PL emission peak. When cadmium stearate was used as Cd precursor (R_1, R_3), independent nucleation occurred as indicated by the appearance of two emission peaks corresponding to CdSe and Zn–Cd–S QDs, respectively. When activated Se and S sources (TOP-Se, TOP-S) were adopted (R_2), independent nucleation can be avoided, but the spectral width of the resulting QDs is significant broader than those prepared with use of elemental Se and S (41 vs 30 nm). These results reveal that the rather abrupt activation of CdO at a certain elevated temperature (herein 150–160 °C) plays a crucial effect on heterogeneous nucleation and growth of monodisperse QDs and avoiding the independent nucleation of shell materials.[52] The role of abrupt activation of CdO is similar as a rapid injection, which is the rate-limiting step for synthesis of nanocrystals in the injection approach. Similar result has been reported for the noninjection synthesis of binary CdS NCs, wherein the reduction of elemental sulfur by ODE, instead of nucleation of the NCs, was likely the

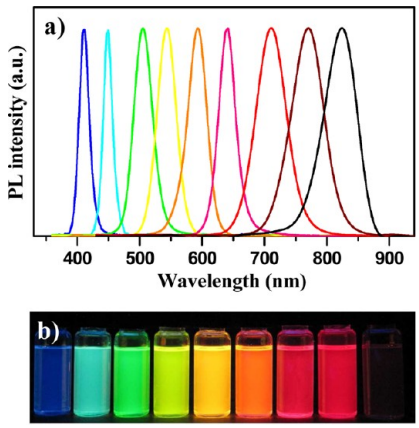

Figure 6. (a) PL emission spectra of obtained core/shell QDs with emission wavelength spanning from violet to NIR window. (b) Photographs of typical emission colors from the obtained QDs under the irradiation of a UV lamp.

rate-limiting step for formation of monodisperse nanocrystals.[53]

General Synthetic Approach for Tuning Emission Color from Violet to NIR. A desired synthetic approach should provide high-quality QDs with emission wavelength range as wide as possible.[36] To the best of our knowledge, very few synthetic approaches have the versatility for preparation of II–VI group core/shell QDs with emission wavelength covering from violet to NIR. Based on the reported single-step noninjection approach, the emission wavelength of CdSe/$Zn_xCd_{1-x}S$ system can be conveniently tuned from 500 to 680 nm with the variation of the amounts of TOP and SA, the nature of zinc sources, as described in Materials and Methods. The reported single-step noninjection synthetic strategy is also workable for the preparation of high-quality CdS-, and CdTe-based core/shell QD systems, and accordingly violet-blue-, and NIR-emissions can be obtained. Table S1 summarizes the experimental conditions and corresponding properties for core/shell QDs with emission wavelength ranging from violet to NIR and the representative TEM images are shown in Figure S3. Violet and blue emissions with wavelength centered at 410 and 460 nm can be facilely obtained *via* the reaction between CdO and elemental S in ODE media containing SA with or without the presence of $Zn(OAc)_2$. When Se was replaced by equal amount of Te, CdTe/$Zn_xCd_{1-x}S$ QDs were then formed with corresponding emission wavelength located in NIR window from 650 to 825 nm. Figure 6 shows the PL spectra ranging from violet to NIR and representative emission colors in the visible spectral window from core/shell QDs prepared by the single-step noninjection synthetic approach.

High Stability. The stability of PL emission, especially in aqueous media, determines the practical applications of QDs in LED and biolabeling.[1–6] The high PL QYs of the obtained core/shell QDs can be preserved for more than one year at ambient atmosphere when

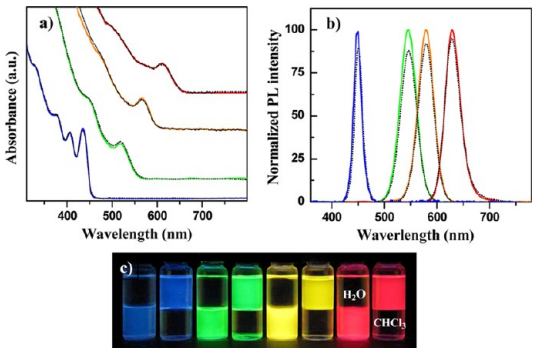

Figure 7. UV–vis absorption (a) and PL emission (b) spectra of representative core/shell structured QDs before (solid curves) and after (dotted curves) phase transfer with use of adenosine monophosphate as phase transfer agent. (c) Photographs of emission colors for QD samples dispersed in H_2O and $CHCl_3$ media under UV irradiation.

dispersed in common nonpolar solvents. More interesting and important, the high PL QYs of the initial oil-soluble QDs can also be retained when the original oil dispersible QDs are transferred into aqueous media through ligand replacement (detailed procedure in Materials and Methods).[54] It was found that after phase transfer, the QDs aqueous solutions exhibited identical absorption and PL emission spectral profiles to those of initial hydrophobic QD dispersions in chloroform (Figure 7a,b). The original high fluorescent brightness was preserved for all selected QDs samples with different emission colors after the phase transfer, and the water-soluble QDs showed more than 90% PL intensity of the initial oil-soluble ones. This is further demonstrated by the almost no distinguishable luminescence brightness of the selected QD samples before and after phase transfer (Figure 7c). It should be noted that heavy loss of luminescence brightness of QDs after phase transfer into aqueous solutions was commonly observed due to the leakage of exciton into the surrounding in previous reports.[14,15,55] The high luminescence of the CdSe/$Zn_xCd_{1-x}S$ in aqueous media can retain for several months without observable quenching. This high PL stability of the water-soluble NIR emitting QDs renders them of special interest in biomedical labeling.[2,3]

Reproducible Large-Scale Synthesis. In the synthesis of luminescent QDs, the particle size and corresponding optical properties (such as PL QY and emission wavelength) of the obtained QDs are usually very sensitive to reaction temperature and growth time in most synthetic approaches.[35–48] This renders the desired optical features are difficult to be captured and thus the reactions lack high reproducibility. While, in our reported single-step noninjection approach, long-term fixation of PL properties (PL peak position, peak width, and PL QY) of the obtained core/shell QDs are observed as described above. This feature favors the capture of desired emission wavelength. Moreover, the emission wavelength of the final QDs is mainly

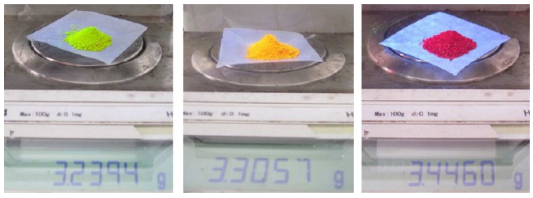

Figure 8. Photographs of dried powder sample of green, yellow, and red emission QDs prepared in a single batch reaction.

determined by the feed ratio of reactants. That is to say, QDs with different emission colors can be achieved by simply changing the synthetic recipe with predetermined amounts of reaction reactants. These features make our reported synthetic approach very reproducible for the preparation of high-quality luminescent QDs with desired emission wavelength spanning the whole visible spectrum and extending to NIR window. Experimental results (Figure S4) show that when we repeated the synthetic experiment 10 times, the PL wavelengths and corresponding QYs of the final QDs were subjected to fluctuations with relative deviation less than 5%. Owing to all reactants were loaded at room temperature, no formation of gas in the reaction process, the reported approach can be readily scaled up for industrial production. We scaled the amount of all reactants up to ~10-fold in a 500 mL three-necked flask. More than 3 g of green, yellow, and red emissive core/shell QDs can be obtained in one bath reaction as shown in Figure 8. Therefore, the reported single-step noninjection synthesis route aiming at producing high quality core/shell QDs for potential industrial applications are scalable, reproducible, and low cost, while enabling the production of QDs in a high yield.

CONCLUSIONS

We have developed a single-step noninjection scalable synthetic approach to prepare high-quality core/shell structured QDs by directly heating commercial available, low-cost, air-stable CdO, $Zn(NO_3)_2$, elemental Se, S/Te in ODE media containing certain amount of TOP and SA. This synthetic approach can be applied for the preparation of CdS/$Zn_xCd_{1-x}S$, CdSe/$Zn_xCd_{1-x}S$, and CdTe/$Zn_xCd_{1-x}S$ core/shell QD systems with corresponding emission wavelength tunable from violet to NIR window. The shell material with gradient alloy structure relieves the strain caused by the lattice mismatch in the core/shell interface, and thus leads to high QY of the QDs. The emission wavelength can be feasibly tuned *via* variation of reaction recipes. The key to the success of this approach is the selection reactants, especially the direct use of CdO as Cd source. The abrupt activation of CdO at elevated temperature ensures the heterogeneous nucleation and controlled growth of core/shell structured QDs with uniform size and chemical composition. The absence of the operation of precursor injection and pyrophoric agents ensures the scalability of the preparation method. This synthetic approach can satisfy the low-cost, reproducible, and scalable requirement for industrial production of high quality core/shell QDs for potential applications.

MATERIALS AND METHODS

Chemicals. Cadmium oxide (CdO, 99.99+%), zinc nitrate hexahydrate ($Zn(NO_3)_2 \cdot 6H_2O$, 98%), zinc acetate ($Zn(OAc)_2$, 99.99%), sulfur powder (S, 99.98%), selenium powder (Se, 100 mesh, ≥ 99.5%), tellurium powder (Te, 200 mesh, 99.8%), 1-octadecene (ODE, 90%), stearic acid (SA, 95%), and trioctylphosphine (TOP, 90%) were purchased from Aldrich. All chemicals were used as received without any further purification. All solvents were obtained from commercial sources and used as received.

Synthesis of CdSe/$Zn_xCd_{1-x}S$ QDs with Emission Wavelength Tunable for 500–680 nm. In a typical synthesis, CdO (0.205 g, 1.6 mmol), $Zn(NO_3)_2 \cdot 6H_2O$ (0.238 g, 0.8 mmol), Se (0.032 g, 0.4 mmol), and S (0.026 g, 0.8 mmol) together with 3.0 mL of TOP, 1.14 g (4 mmol) of SA were mixed with 20 mL of 1-octadecene (ODE) in a 100 mL three-necked flask. The flask was fitted with a heating mantle, a condenser, and a temperature probe and placed on a stirplate. The mixture was then heated to 250 °C at a heating rate of 20–40 °C/min under air with vigorous stirring. During the reaction, aliquots were taken with a syringe at different times to monitor the growth of QDs by recording UV–vis absorption and PL emission spectra. Afterward, the reaction solution was cooled to ~80 °C and precipitated by ethanol. Further purification by centrifugation and decantation was carried out use of $CHCl_3$/ethanol mixture solvent. Finally, the products were redispersed in toluene or chloroform or dried under vacuum for further analyses. A total of 0.35 g of dried product with an emission wavelength around 625 nm can be obtained.

In the case of $Zn(NO_3)_2$ used as Zn source, with the variation of the amount of TOP and/or SA, the emission wavelength of the obtained QDs can be conveniently tuned from 500 to 630 nm. For example, with the fixation of other variables, when the amount of TOP was varied from 0 to 0.4 mL, the emission wavelength can be tuned from 500 to 550 nm. With fixation of TOP at 0.4 mL, when SA amount was varied from 4.0 to 6.0 mmol, the emission wavelength can be tuned from 550 to 600 nm. When $Zn(NO_3)_2$ was replaced by $Zn(OAc)_2$, with the variation of SA from 4.0 to 2.0 mmol, the corresponding emission wavelength can be tuned from 620 to 680 nm.

Synthesis of Red- to NIR-Emitting CdTe/$Zn_xCd_{1-x}S$ Core/Shell QDs. In a typical synthesis, CdO (0.205 g, 1.6 mmol), $Zn(OAc)_2$ (0.128 g, 0.8 mmol), Te (0.051 g, 0.4 mmol), and S (0.026 g, 0.8 mmol) together with 3.0 mL of TOP, 1.14 g of SA were mixed with 20 mL of ODE in a 100 mL three-necked flask. The mixture was then degassed at room temperature for 10 min. After that, the solution was heated to 250 °C at a heating rate of 20–40 °C/min under N_2 flow with vigorous stirring. The following monitoring and purification operations were similar to those of CdSe/$Zn_xCd_{1-x}S$ QDs described above. 0.37 g of dried QD products can be obtained. With the variation of reaction temperature (230–250 °C)) and reaction time (0–30 min), the emission wavelength of the obtained QDs can be conveniently tuned from 650 to 825 nm.

Synthesis of Blue-Emitting CdS/$Zn_xCd_{1-x}S$ Core/Shell QDs. In a typical synthesis, CdO (0.205 g, 1.6 mmol), $Zn(OAc)_2$ (0.128 g, 0.8 mmol), and S (0.026 g, 0.8 mmol) together with 1.14 g of SA were mixed with 20 mL of ODE in a 100 mL three-necked flask. The mixture was then degassed at room temperature for 10 min. After that,

the solution was heated to 250 °C at a heating rate of 20−40 °C/min under N_2 flow with vigorous stirring. A total of 0.33 g of dried QD product can be obtained. With the variation of the amount of $Zn(OAc)_2$ (0−0.8 mmol), the emitting wavelength of the obtained QDs can be tuned from 410 to 450 nm.

Ligand Exchange. Exchange of the native hydrophobic ligands on QDs surface by adenosine monophosphate (AMP) was performed as follows. Typically, 1.0 g (2.74 mmol) of AMP was dissolved in 3.0 mL of ethanol, and the pH of the resulting solution was adjusted to 10 with the use of concentrated NaOH solution. Then 0.3 mL of the obtained AMP solution (containing 0.27 mmol AMP) in ethanol was added dropwise into a purified QDs solution in $CHCl_3$ (containing 1×10^{-6} M QDs, 20.0 mL) and vigorously stirred for 30 min. Subsequently, deionized water was added into the solution. The QDs were found to be successfully transferred from the organic phase on the bottom to the aqueous phase in the top. The colorless organic phase was discarded and the aqueous phase containing the QDs was collected. The excess amount of free ligand was removed by centrifugation purification with use of acetone. The supernatant was discarded and the pellet was then redissolved in water and repeated this centrifugation−decantation process three times to get the purified QDs aqueous solutions.

Gram-Scale Production of CdSe/$Zn_xCd_{1-x}S$ QDs. For the preparation of gram-scale red-emitting CdSe/$Zn_xCd_{1-x}S$ QDs, CdO (2.05 g, 16 mmol), $Zn(NO_3)_2 \cdot 6H_2O$ (2.38 g, 8 mmol), Se (0.32 g, 4 mmol), and S (0.26 g, 8 mmol) together with 30 mL of TOP, 11.4 g SA was mixed with 150 mL of 1-octadecene (ODE) in a 500 mL three-necked flask. The mixture was then heated to 250 °C at a heating rate of 20−40 °C/min under air with vigorous stirring and kept at this temperature for 1 h. The QDs were then obtained and purified *via* a routine process elaborated above. For the preparation of green-emitting QDs, all other variables were the same as for the red ones, while the amount of TOP was changed to 3.0 mL. For the preparation of yellow-emitting QDs, the amount of TOP was changed to 3.0 mL, and SA was changed to 17.2 g. For all QD samples, more than 3 g of dried products were obtained.

Characterization. UV−vis and PL spectra were obtained on a Shimadzu UV-2450 spectrophotometer and a Cary Eclipse (Varian) fluorescence spectrophotometer, respectively. The room-temperature PL QY was determined by comparing the integrated emission of the QDs samples in chloroform with that of a fluorescent dye (such as rhodamine 6 G with QY of 95% or rhodamine 640 with QY of 100%) in ethanol with identical optical density. A quadratic refractive index correction was done in order to compensate the different refractive index of the different solvents used for organic dyes and QDs. Also, the known QYs of the QDs in solution can be used to measure the PL efficiencies of other QDs by comparing their integrated emission.

To conduct investigations in the transmission electron microscopy (TEM), the QDs were deposited from dilute toluene solutions onto copper grids with carbon support by slowly evaporating the solvent in air at room temperature. TEM and high resolution (HR) TEM images were acquired using a JEOL JEM-2010 transmission electron microscope (operating at an acceleration voltage of 200 kV), which is equipped with an energy-dispersive X-ray (EDX) detector that was used for elemental analysis. Powder X-ray diffraction (XRD) was obtained by wide-angle X-ray scattering, using a Siemens D5005 X-ray powder diffractometer equipped with graphite monochromatized Cu Kα radiation (λ = 1.5406 Å). XRD samples were prepared by depositing NC powder on a piece of Si (100) wafer. The composition for the QDs was measured by means of inductively coupled plasma atomic emission spectroscopy (ICP-AES, Thermo Elemental IRIS 1000) using a standard HCl/HNO_3 digestion with addition of few drops of H_2O_2.

Conflict of Interest: The authors declare no competing financial interest.

Acknowledgment. The work was supported by National Natural Science Foundation of China (No. 21175043), the Science and Technology Commission of Shanghai Municipality (11JC1403100, 12NM0504101, 12ZR1407700), and the Fundamental Research Funds for the Central Universities for financial support.

Supporting Information Available: XRD pattern, EDX spectrum, TEM images, experimental reproducibility, and synthetic conditions and the corresponding PL features of representative QDs. This material is available free of charge *via* the Internet at http://pubs.acs.org.

REFERENCES AND NOTES

1. Talapin, D. V.; Lee, J. S.; Kovalenko, M. V.; Shevchenko, E. V. Prospects of Colloidal Nanocrystals for Electronic and Optoelectronic Applications. *Chem. Rev.* **2010**, *110*, 389–458.
2. Zrazhevskiy, P.; Sena, M.; Gao, X. Designing Multifunctional Quantum Dots for Bioimaging, Detection, and Drug Delivery. *Chem. Soc. Rev.* **2010**, *39*, 4326–4354.
3. Kamat, P. V.; Tvrdy, K.; Baker, D. R.; Radich, J. G. Beyond Photovoltaics: Semiconductor Nanoarchitectures for Liquid-Junction Solar Cells. *Chem. Rev.* **2010**, *110*, 6664–6688.
4. Pan, Z.; Zhang, H.; Cheng, K.; Hou, Y.; Hua, J.; Zhong, X. Highly Efficient Inverted Type-I CdS/CdSe Core/Shell Structure QD-Sensitized Solar Cells. *ACS Nano* **2012**, *6*, 3982–3991.
5. Kramer, I. J.; Sargent, E. H. Colloidal Quantum Dot Photovoltaics: A Path Forward. *ACS Nano* **2011**, *5*, 8506–8514.
6. Rogach, A. L.; Gaponik, N.; Lupton, J. M.; Bertoni, C.; Gallardo, D. E.; Dunn, S.; Pira, N. L.; Paderi, M.; Repetto, P.; Romanov, S. G.; O'Dwyer, C.; Torres, C. M. S.; Eychmuller, A. Light-Emitting Diodes with Semiconductor Nanocrystals. *Angew. Chem., Int. Ed.* **2008**, *47*, 6538–6549.
7. Reiss, P.; Protiere, M.; Li, L. Core/Shell Semiconductor Nanocrystals. *Small* **2009**, *5*, 154–168.
8. Regulacio, M. D.; Han, M. Y. Composition-Tunable Alloyed Semiconductor Nanocrystals. *Acc. Chem. Res.* **2010**, *43*, 1025–1102.
9. Pradhan, N.; Sarma, D. D. Advances in Light-Emitting Doped Semiconductor Nanocrystals. *J. Phys. Chem. Lett.* **2011**, *2*, 2818–2826.
10. Hines, M. A.; Guyot-Sionnest, P. Synthesis and Characterization of Strongly Luminescing ZnS-Capped CdSe Nanocrystals. *J. Phys. Chem.* **1996**, *100*, 468–471.
11. Dabbousi, B. O.; Rodriguez-Viejo, J.; Mikulec, F. V.; Heine, J. R.; Mattoussi, H.; Ober, R.; Jensen, K. F.; Bawendi, M. G. (CdSe)ZnS Core−Shell Quantum Dots: Synthesis and Characterization of a Size Series of Highly Luminescent Nanocrystallites. *J. Phys. Chem. B* **1997**, *101*, 9463–9475.
12. Cao, Y.; Banin, U. Growth and Properties of Semiconductor Core/Shell Nanocrystals with InAs Cores. *J. Am. Chem. Soc.* **2000**, *122*, 9692–9702.
13. Talapin, D. V.; Rogach, A. L.; Kornowski, A.; Hasse, M.; Weller, H. Highly Luminescent Monodisperse CdSe and CdSe/ZnS Nanocrystals Synthesized in a Hexadecylamine-Trioctylphosphine Oxide-Trioctylphospine Mixture. *Nano Lett.* **2001**, *1*, 207–211.
14. Reiss, P.; Bleuse, J.; Pron, A. Highly Luminescent CdSe/ZnSe Core/Shell Nanocrystals of Low Size Dispersion. *Nano Lett.* **2002**, *2*, 781–784.
15. Li, J. J.; Wang, Y. A.; Guo, W.; Keay, J. C.; Mishima, T. D.; Johnson, M. B.; Peng, X. Large-Scale Synthesis of Nearly Monodisperse CdSe/CdS Core/Shell Nanocrystals Using Air-Stable Reagents *via* Successive Ion Layer Adsorption and Reaction. *J. Am. Chem. Soc.* **2003**, *125*, 12567–12575.
16. Mekis, I.; Talapin, D. V.; Kornowski, A.; Haase, M.; Weller, H. One-Pot Synthesis of Highly Luminescent CdSe/CdS Core−Shell Nanocrystals *via* Organometallic and "Greener" Chemical Approaches. *J. Phys. Chem. B* **2003**, *107*, 7454–7462.
17. Xie, R.; Kolb, U.; Li, J.; Basche, T. Synthesis and Characterization of Highly Luminescent CdSe−Core CdS/$Zn_{0.5}Cd_{0.5}S$/ZnS Multishell Nanocrystals. *J. Am. Chem. Soc.* **2005**, *127*, 7480–7488.
18. Kim, J. I.; Lee, J.-K. Sub-Kilogram-Scale One-Pot Synthesis of Highly Luminescent and Monodisperse Core/Shell Quantum Dots by the Successive Injection of Precursors. *Adv. Funct. Mater.* **2006**, *16*, 2077–2082.

19. Xie, R.; Peng, X. Synthetic Scheme for High-Quality InAs Nanocrystals Based on Self-Focusing and One-Pot Synthesis of InAs-Based Core-Shell Nanocrystals. *Angew. Chem., Int. Ed.* **2008**, *47*, 7677–7680.
20. Mahler, B.; Spinicelli, P.; Buil, S.; Quelin, X.; Hermier, J.-P.; Dubertret, B. Towards Non-Blinking Colloidal Quantum Dots. *Nature mater.* **2008**, *7*, 659–664.
21. Zhang, W.; Chen, G.; Wang, J.; Ye., B.-C.; Zhong, X. Design and Synthesis of Highly Luminescent Near-Infrared-Emitting Water-Soluble CdTe/CdSe/ZnS Core/Shell/Shell Quantum Dots. *Inorg. Chem.* **2009**, *48*, 9723–9731.
22. van Embden, J.; Jasieniak, J.; Mulvaney, P. Mapping the Optical Properties of CdSe/CdS Heterostructure Nanocrystals: The Effects of Core Size and Shell Thickness. *J. Am. Chem. Soc.* **2009**, *131*, 14299–14309.
23. Smith, A. M.; Mohs, A. M.; Nie, S. Tuning the Optical and Electronic Properties of Colloidal Nanocrystals by Lattice Strain. *Nat. Nanotechnol.* **2009**, *4*, 56–63.
24. Allen, P. M.; Liu, W.; Chauhan, V. P.; Lee, J.; Ting, A. Y.; Fukumura, D.; Jain, R. K.; Bawendi, M. G. InAs(ZnCdS) Quantum Dots Optimized for Biological Imaging in the Near-Infrared. *J. Am. Chem. Soc.* **2010**, *132*, 470–471.
25. Dethlefsen, J. R.; Dossing, A. Preparation of a ZnS Shell on CdSe Quantum Dots Using a Single-Molecular ZnS Precursor. *Nano Lett.* **2011**, *11*, 1964–1969.
26. Liu, W.; Choi, H. S.; Zimmer, J. P.; Tanaka, E.; Frangioni, J. V.; Bawendi, M. Compact Cysteine-Coated CdSe(ZnCdS) Quantum Dots for *In Vivo* Applications. *J. Am. Chem. Soc.* **2007**, *129*, 14530–14531.
27. Murray, C. B.; Norris, D. J.; Bawendi, M. G. Synthesis and Characterization of Nearly Monodisperse CdE (E = S, Se, Te) Semiconductor Nanocrystallites. *J. Am. Chem. Soc.* **1993**, *115*, 8706–8715.
28. Hines, M. A.; Guyot-Sionnest, P. Bright UV Blue Luminescent Colloidal ZnSe Nanocrystals. *J. Phys. Chem. B* **1998**, *102*, 3655–3657.
29. Peng, Z. A.; Peng, X. Formation of High-Quality CdTe, CdSe, and CdS Nanocrystals Using CdO as Precursor. *J. Am. Chem. Soc.* **2001**, *123*, 183–184.
30. Qu, L.; Peng, Z. A.; Peng, X. Alternative Routes Toward High Quality CdSe Nanocrystals. *Nano Lett.* **2001**, *1*, 333–337.
31. Yu, W. W.; Peng, X. Formation of High-Quality CdS and Other II–VI Semiconductor Nanocrystals in Noncoordinating Solvents: Tunable Reactivity of Monomers. *Angew Chem., Int. Ed.* **2002**, *41*, 2368–2371.
32. Kairdolf, B. A.; Smith, A. M.; Nie, S. One-Pot Synthesis, Encapsulation, and Solubilization of Size-Tuned Quantum Dots with Amphiphilic Multidentate Ligands. *J. Am. Chem. Soc.* **2008**, *130*, 12866–12867.
33. de Mello Donega, C.; Hickey, S. G.; Wuister, S. F.; Vanmaekelbergh, D.; Meijerink, A. Single-Step Synthesis to Control the Photoluminescence Quantum Yield and Size Dispersion of CdSe Nanocrystals. *J. Phys. Chem. B* **2003**, *107*, 489–496.
34. Deng, Z.; Cao, L.; Tang, F.; Zou, B. A New Route to Zinc-Blende CdSe Nanocrystals: Mechanism and Synthesis. *J. Phys. Chem. B* **2005**, *109*, 16671–16675.
35. Zhong, X.; Feng, Y.; Zhang, Y. Facile and Reproducible Synthesis of Red-Emitting CdSe Nanocrystals in Amine with Long-Term Fixation of Particle Size and Size Distribution. *J. Phys. Chem. C* **2007**, *111*, 526–531.
36. Gaponik, N.; Hickey, S. G.; Dorfs, D.; Rogach, A. L.; Eychmuller, A. Progress in the Light Emission of Colloidal Semiconductor Nanocrystals. *Small* **2010**, *6*, 1364–1378.
37. Liu, J. H.; Fan, J. B.; Gu, Z.; Cui, J.; Xu, X. B.; Liang, Z. W.; Luo, S. L.; Zhu, M. Q. *Langmuir* **2008**, *24*, 5241–5244.
38. Protiere, M.; Nerambourg, N.; Renard, O.; Reiss, P. Rational Design of the Gram-Scale Synthesis of Nearly Monodisperse Semiconductor Nanocrystals. *Nanoscale Res Lett.* **2011**, *6*, 472.
39. Kwon, S. G.; Hyeon, T. Formation Mechanisms of Uniform Nanocrystals *via* Hot- Injection and Heat-Up Methods. *Small* **2011**, *7*, 2685–2702.
40. Cao, Y. C.; Wang, J. H. One-Pot Synthesis of High-Quality Zinc-Blende CdS Nanocrystals. *J. Am. Chem. Soc.* **2004**, *126*, 14336–14337.
41. Li, L.; Reiss, P. One-Pot Synthesis of Highly Luminescent InP/ZnS Nanocrystals without Precursor Injection. *J. Am. Chem. Soc.* **2008**, *130*, 11588–11589.
42. Zhong, H.; Lo, S. S.; Mirkovic, T.; Li, Y.; Ding, Y.; Li, Y.; Scholes, G. D. Noninjection Gram-Scale Synthesis of Monodisperse Pyramidal $CuInS_2$ Nanocrystals and Their Size-Dependent Properties. *ACS Nano* **2010**, *4*, 5253–5262.
43. Kwon, S. G.; Piao, Y.; Park, J.; Angappane, S.; Jo, Y.; Hwang, N.-M.; Park, J.-G.; Hyeon, T. Kinetics of Monodisperse Iron Oxide Nanocrystal Formation by "Heating-Up" Process. *J. Am. Chem. Soc.* **2007**, *129*, 12571–12584.
44. Sun, S. H.; Murray, C. B.; Weller, D.; Folks, L.; Moser, A. Monodisperse FePt nanoparticles and ferromagnetic FePt nanocrystal superlattices. *Science* **2000**, *287*, 1989–1992.
45. Zhong, X.; Zhang, Z.; Liu, S.; Han, M.; Knoll, W. Embryonic Nuclei-Induced Alloying Process for the Reproducible Synthesis of Blue-Emitting $Zn_xCd_{1-x}Se$ Nanocrystals with Long-Time Thermal Stability in Size Distribution and Emission Wavelength. *J. Phys. Chem. B* **2004**, *108*, 15552–15559.
46. Bae, W. K.; Char, K.; Hur, H.; Lee, S. Single-Step Synthesis of Quantum Dots with Chemical Composition Gradients. *Chem. Mater.* **2008**, *20*, 531–539.
47. Deng, Z.; Yan, H.; Liu, Y. Band Gap Engineering of Quaternary-Alloyed ZnCdSSe Quantum Dots *via* a Facile Phosphine-Free Colloidal Method. *J. Am. Chem. Soc.* **2009**, *131*, 17744–17745.
48. Cho, J.; Jung, Y. K.; Lee, J.-K. Kinetic Studies on the Formation of Various II–VI Semiconductor Nanocrystals and Synthesis of Gradient Alloy Quantum Dots Emitting in the Entire Visible Range. *J. Mater. Chem.* **2012**, *22*, 10827–10833.
49. Zhong, X.; Han, M.; Dong, Z.; White, T. M.; Knoll, W. Composition-Tunable $Zn_xCd_{1-x}Se$ Nanocrystals with High Luminescence and Stability. *J. Am. Chem. Soc.* **2003**, *125*, 8589–8594.
50. Maikov, G. I.; Vaxenburg, R.; Sashchiuk, A.; Lifshitz, E. Composition-Tunable Optical Properties of Colloidal IV–VI Quantum Dots, Composed of Core/Shell Heterostructures with Alloy Components. *ACS Nano* **2010**, *4*, 6547–6556.
51. Sarma, D. D.; Nag, A.; Santra, P. K.; Kumar, A.; Sapra, S.; Mahadevan, P. Origin of the Enhanced Photoluminescence from Semiconductor CdSeS Nanocrystals. *J. Phys. Chem. Lett.* **2010**, *1*, 2149–2153.
52. Owen, J. S.; Chan, E. M.; Liu, H.; Alivisatos, A. P. Precursor Conversion Kinetics and the Nucleation of Cadmium Selenide Nanocrystals. *J. Am. Chem. Soc.* **2010**, *132*, 18206–18213.
53. Li, Z.; Ji, Y.; Xie, R.; Grisham, S. Y.; Peng, X. Correlation of CdS Nanocrystal Formation with Elemental Sulfur Activation and Its Implication in Synthetic Development. *J. Am. Chem. Soc.* **2011**, *133*, 17248–17256.
54. Liu, L.; Zhong, X. A General and Reversible Phase Transfer Strategy Enabling Nucleotides Modified High-Quality Water-Soluble Nanocrystals. *Chem. Commun.* **2012**, *48*, 5718–5720.
55. Pellegrino, T.; Mann, L.; Kudera, S.; Liedl, T.; Koktysh, D.; Rogach, A. L.; Keller, S.; Radler, J.; Natile, G.; Parak, W. J. Hydrophobic Nanocrystals Coated with An Amphiphilic Polymer Shell: A General Route to Water Soluble Nanocrystals. *Nano Lett.* **2004**, *4*, 703–707.